

## Measurements of Symmetric Vortex Merger

K. S. Fine, C. F. Driscoll, J. H. Malmberg, and T. B. Mitchell

University of California at San Diego, La Jolla, California 92093

(Received 11 March 1991)

Magnetically confined columns of electrons are excellent experimental realizations of extended two-dimensional vortices in an inviscid fluid. Here, we consider two nearly identical vortices orbiting around one another inside a cylindrical wall. The vortices merge symmetrically, in a time which varies from less than 1 to about  $10^4$  orbit periods as the vortex separation is increased by 30%. We have obtained images of the vorticity distribution during this merger process, and observe filamentary tails and mixing. These experimental results are consistent with analytic models and numerical simulations.

PACS numbers: 47.15.Ki, 52.25.Wz

The dynamics of two-dimensional vortices in an inviscid, ideal fluid has been the subject of theoretical investigation for over a century [1]. In recent years, the merging of extended vortices with the same sign of vorticity has been proposed as a key element in the decay of turbulence in 2D flows [2]. In particular, the simple case of the interaction of two symmetric vortices has been the subject of analytic models and computer simulations [3–6]. Experiments with conventional fluids have observed merger [7], but are complicated by the presence of radial and axial boundary layers and other effects not included in the 2D fluid model [8].

In this Letter, we describe vortex merger experiments using electron plasmas as experimental manifestations of ideal 2D fluids. The electron system has no boundary layers to dissipate the vortices, and shows little dissipation even on time scales of  $10^4$  orbits. The electron system may thus offer the best experimental data on this fundamental vortex interaction process. More generally, this non-neutral plasma system [9] offers experimental insight into shear-induced vortex generation, dynamics, and dissipation [10] which may affect cross-field transport in neutral plasmas [11].

We have observed that two electron plasma vortices orbit around each other for up to  $10^4$  orbits before merging. The time for merger decreases by 4 orders of magnitude when the separation is decreased from 1.8 to 1.4 vortex diameters. We have made detailed measurements of the plasma vorticity  $\Omega(r, \theta)$  during the merger process and have observed the formation of filamentary tails and mixing that have also been seen in computer simulations.

The electron columns discussed here are contained in a series of grounded conducting cylinders, as shown in Fig. 1. A uniform axial magnetic field ( $B = 375$  G) provides radial confinement, and negative voltages applied to end cylinders provide axial confinement. The apparatus is operated in an inject-manipulate-dump cycle. For injection, the leftmost cylinder is briefly grounded, allowing electrons to enter from the negatively biased tungsten filament source. The trapped electrons can then be manipulated by applying voltages to various sections of the cylindrical wall. Typically, we manipulate the plasma to create the desired “initial condition,” then study the re-

sulting evolution.

At any time  $t$  during the evolution, we can obtain the  $z$ -averaged electron density  $n(r, \theta, t)$  by grounding the rightmost cylinder, thereby dumping the electrons. We measure the charge  $Q(r, \theta, t)$  which flows along  $B$  through a collimator hole of area  $A_h = \pi(1.6 \text{ mm})^2$ , giving

$$n(r, \theta, t) \equiv Q(r, \theta, t) / (-eA_h L) \\ = \int dz \tilde{n}(r, \theta, z, t) / L, \quad (1)$$

where  $L$  is the column length. Additionally, the total charge dumped is measured. Only one density measurement is obtained on each machine cycle. We obtain the temporal dependence by varying the evolution time  $t$ ; and the spatial dependence by varying the position  $r$  of the radially scanning collimator hole, and the phase  $\theta$  of the initial condition. Of course, this imaging process relies on a high shot-to-shot reproducibility in the plasma initial conditions; typically we have less than 1% shot-to-shot variation in the measured  $Q$  at  $t = 0$ .

The electron columns considered here have local densities  $\tilde{n} \approx (1-4) \times 10^6 \text{ cm}^{-3}$  out to a radius  $R_r \approx 0.5-1.0$  cm over an axial length  $L \approx 15-50$  cm, and are contained in a cylinder of radius  $R_w = 3.81$  cm. The unneutralized space charge gives a radial electric field  $E_r < -3$  V/cm, so the column has an  $E \times B$  rotation frequency of  $f_E < 140$  kHz. The initially injected electrons have a

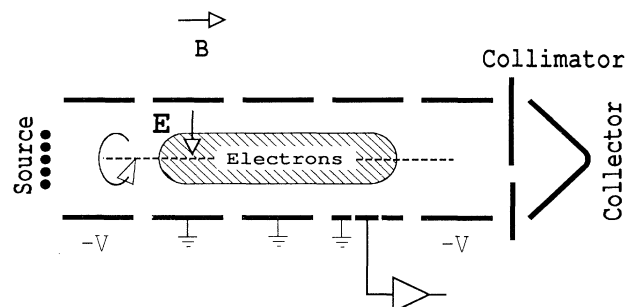


FIG. 1. Schematic diagram of the cylindrical containment system.

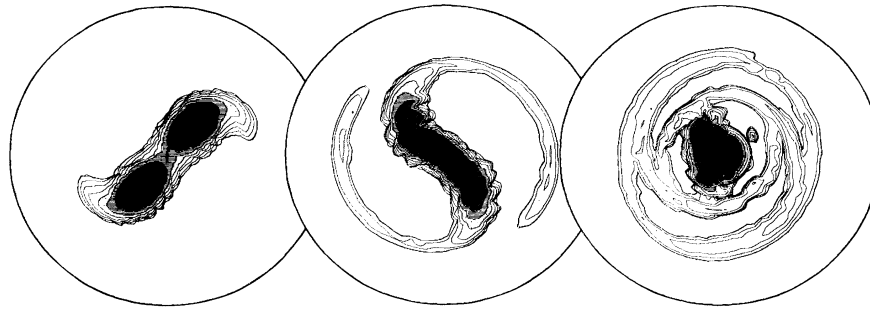


FIG. 2. Measured contour plots of density (or vorticity) during vortex merger. The three pictures are separated by 30- $\mu$ sec intervals, and the eight contours are on a logarithm scale spanning 1 to 0.01. The outer circles represent the conducting wall.

characteristic thermal energy  $kT \approx 0.1-1.0$  eV, giving a cyclotron radius  $r_c < 60 \mu\text{m}$ . Subsequent manipulations may increase the parallel temperature 1-2 eV, giving axial bounce rates  $f_b \gtrsim 10f_E$ .

In this parameter regime, the electron dynamics is well approximated by 2D guiding-center theory. Here, the axial bouncing of the individual electrons averages over any  $z$  variations at a rate fast compared to  $r-\theta$  motions. The  $r-\theta$  dynamics can be calculated by treating the electrons as a continuous fluid of guiding centers with density  $n(r, \theta)$  and velocity  $\mathbf{v}(r, \theta) = c\mathbf{E}(r, \theta) \times \hat{\mathbf{z}}/B$ . Poisson's equation determines the electric field  $\mathbf{E}$  from the electron density and the applied wall voltages.

The 2D drift Poisson equations for the evolution of the electron column are isomorphic to the 2D Euler equations for an inviscid fluid of uniform density [12,13]. Thus, in this approximation, the electron columns evolve the same as columns of vorticity in an idealized fluid. The electric potential  $\phi(r, \theta)$  is isomorphic to the fluid stream function  $\psi(r, \theta)$ . In the electron case, the vorticity of the flow is proportional to the electron density, i.e.,  $\Omega \equiv \nabla \times \mathbf{v} \propto \nabla^2 \phi \propto n$ . A centered, symmetric vortex will have a stationary flow field  $v_\theta(r)$ , with  $v_\theta \propto 1/r$  outside the region of vorticity; this arises naturally in the electron system, since  $E_r \propto 1/r$  outside the electron column.

We have studied the evolution of two equal electron columns placed at the same radius and  $180^\circ$  apart in the cylindrical system. To create this initial condition, a centered vortex is drifted a distance  $D$  off center, using voltages applied to azimuthal sections of the wall. This displaced column orbits around the central axis, due to interaction with the image charges in the wall. Next, the column is cut in half longitudinally by applying a negative voltage to the central cylindrical section (which was previously grounded). The two columns are then "dephased" in their orbits by changing the containment voltage at one end. When the two columns are  $180^\circ$  out of phase, the central section is again grounded, and the columns expand longitudinally to form two symmetrically placed columns with the same axial extent.

An example of the resulting evolution is shown in Fig. 2. The three contour plots show  $n(r, \theta, t)$  at  $t = 10, 40,$

and  $70 \mu\text{sec}$  after the formation of the two-vortex state. The interaction of the two flow fields causes filamentary tail formation, and we observe vortex merger at the center within one orbit period. The filamentary tails continue wrapping around the central core, eventually forming a low-density extension of the essentially  $\theta$ -symmetric single vortex.

The evolution of the two-vortex state depends critically on the initial separation  $2D$ . This separation can be scaled by the vortex diameter  $2R_v$ , defined by

$$R_v = \frac{3}{2} \int nr' dA/N_L. \tag{2}$$

Here, the integrals are over the area of a single vortex,  $r' \equiv |\mathbf{r} - \mathbf{R}_{c.m.}|$ , with  $\mathbf{R}_{c.m.} \equiv \int nr dA/N_L$  being the "center of mass" of the vortex, and the linear density is given by  $N_L \equiv \int n dA$ . The factor of  $\frac{3}{2}$  is chosen such that a circular patch of constant vorticity with radius  $\rho$  has  $R_v = \rho$ .

The evolution of Fig. 2 is characterized by  $R_v = 0.67$  cm, and  $D/R_v = 1.48$ . If the same vortices are initially separated by  $D/R_v = 1.61$ , then their mutual interaction still results in filamentary tail formation, but the vortices orbit around each other for about 100 orbits before merging at the center. If the vortices are separated by  $D/R_v = 1.8$ , then we observe that they orbit around each other for about  $10^4$  orbits before merging or degrading.

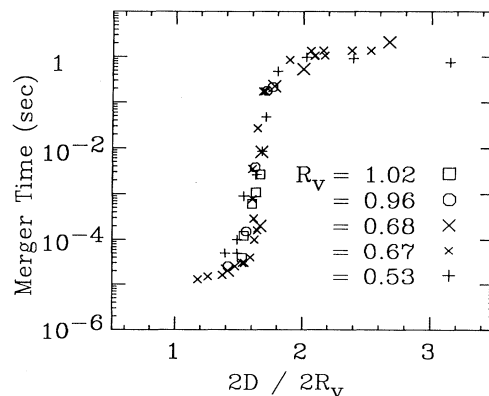


FIG. 3. Measured two-vortex merger time as a function of separation  $2D$  normalized to vortex diameter  $2R_v$ .

Of course, on these long time scales, other processes besides inviscid symmetric merger may be occurring.

Figure 3 plots the time  $\tau_{\text{merge}}$  between the creation of the two-vortex state and merger versus  $D/R_c$  for vortices with radii  $R_c = 0.53, 0.67, 0.68, 0.96,$  and  $1.02$  cm. For short merger times ( $< 500 \mu\text{sec}$ ),  $\tau_{\text{merge}}$  is defined from the density plots as the time where the vortex cores fuse; at longer times,  $\tau_{\text{merge}}$  is defined to be the point at which the two-vortex signal on the wall probe abruptly disappears. It is particularly striking that  $\tau_{\text{merge}}$  increases by 4 orders of magnitude between  $D/R_c = 1.4$  and  $1.8$ .

It is also striking that the curves for different  $R_c$  overlay one another, indicating that  $R_c$  determines the length scale. The wall radius  $R_w$  does not enter the scaling, because wall interactions are negligible for our ranges of  $D$ . We note here that wall effects do become important when  $D \geq R_w/2$ , causing an instability in the orbits of the vortices [14], and we have excluded data in this parameter regime.

The radial density profiles of the initial, centered columns are shown in Fig. 4, with the curves identified by the symbols of Fig. 3. These profiles were used in Eq. (2) to calculate the  $R_c$  values of Fig. 3. We note that these profiles appear similar when rescaled by  $R_c$ ; i.e., our experiments did not vary the profile shapes over a wide range. All columns have length  $L \approx 15$  cm except for the large  $\times$ 's which have  $L \approx 45$  cm. The merger process is seen to be independent of the length of our system.

These results are in good agreement with theory and computational results of two-dimensional ideal fluids. Moore and Saffman [3] used an approximate analytical model for elliptical patches of constant vorticity and find that there are no two-vortex solutions for  $D/R_c < 1.43$ . Numerical solution of an equilibrium equation by Saffman and Szeto [4] predicts a critical separation of  $D/R_c = 1.58$ . Computer simulations by Rossow [5] based upon collections of 36 point vortices give a critical distance of  $D/R_c = 1.7$ , using a definition of  $R_c$  equivalent to

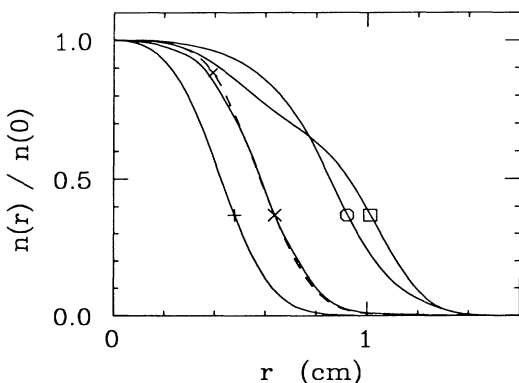


FIG. 4. Measured density (or vorticity) profiles for the columns before merger. The curves are labeled by symbols corresponding to Fig. 3.

Eq. (2). Extensive computer simulations by Melander, Zabusky, and McWilliams [6] also observed merger depending critically on separation distance. These authors have also developed an approximate moment model of the two-vortex interaction.

Experimentally, the coalescence of symmetric vortices was observed in water in a rotating tank by Griffiths and Hopfinger [7]. They observed merger below a critical separation of  $D/R_c \approx 1.6$  for anticyclonic vortices (rotating opposite to the rotation of the tank); but they observed merger in all cases for cyclonic vortices. Since the Euler equation is symmetric with respect to the sign of vorticity, this asymmetry indicates that nonideal or three-dimensional effects were significant [8].

We have also measured the orbital frequency  $f_{\text{orb}}$  of the two-vortex state, as shown in Fig. 5. For vortices corresponding to the  $\times$ 's of Fig. 3, the orbit frequency varies from 8 to 20 kHz over our accessible range of separations. Here, the separation  $2D$  is scaled to the wall diameter  $2R_w$ , for comparison to a simple line charge model. The model predicts

$$f_{\text{orb}} = \frac{ceN_L}{B 2\pi D^2} \left[ 1 - \frac{2}{1 - R_w^2/D^2} - \frac{2}{1 + R_w^2/D^2} \right], \quad (3)$$

shown as the solid curve in Fig. 5. All frequencies scale with  $N_L/B$ ; in fluid notation, this would be the circulation  $\Gamma \equiv \int \Omega dA = 4\pi ceN_L/B$ . The direct interaction of the two vortices gives the leading factor, scaling as  $1/D^2$ . Interaction with the cylindrical wall is equivalent to interaction with two image charges at a radius of  $R_w^2/D$ , giving the two correction terms.

The measured orbit frequencies are uniformly about 2.5 kHz greater than the predictions of Eq. (3), as shown by the dot-dashed curve. We believe that this frequency

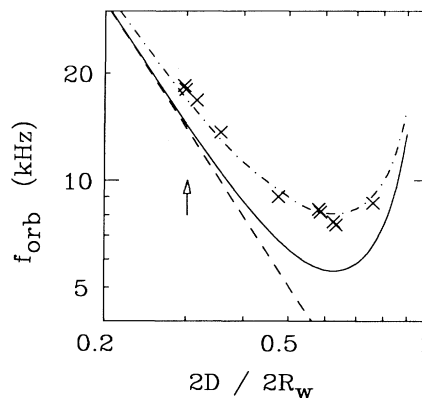


FIG. 5. Measured two-vortex orbit frequency vs separation normalized to wall diameter, for conditions corresponding to the large  $\times$ 's of Fig. 3. The arrow indicates the merger boundary at  $2D/2R_w = 1.6$ . The curves show predicted frequencies with no wall (dashed) and with a wall (solid). The dot-dashed curve is the solid curve offset by 2.5 kHz.

shift is due to the finite length of our system. Essentially, the radial force from the confinement fields at the ends of the columns contributes an  $\mathbf{E} \times \mathbf{B}$  drift in the azimuthal direction. We speculate that when averaged over axial position, this is equivalent to a uniform background vorticity. We believe this has little effect on the merger process since the Euler equations are invariant with respect to a constant offset in vorticity. This frequency shift is also seen in the orbital frequency of a single off-center vortex [15].

The experiments described here demonstrate that the electron system is useful for exploring 2D fluid dynamics. One advantage of the electron experiments is that the electron columns tend to remain 2D due to the magnetic field. Another advantage is that the electron columns have low internal viscosity and have no boundary layers at the cylindrical walls or ends. The time for internal viscosity to act on a global scale is typically 10 sec, compared to the 100- $\mu$ sec time scale for the drift motions of interest here. Further, the  $\mathbf{E} \times \mathbf{B}$  velocity  $v_\theta$  may be large at the wall, but since there are typically no electrons near the walls, one has a free-slip boundary condition. Of course, small effects on the electron dynamics (such as finite-cyclotron-radius and finite-z-length effects) have been ignored here.

In summary, we have studied the dynamics of two symmetric vortices using magnetized electron columns, and have observed vortex merger which depends critically on the separation to vortex diameter ratio. For separations less than 1.4 vortex diameters we see rapid merger accompanied by filamentary tail formation. For separations greater than 1.8 vortex diameters we observe that the two vortices orbit around each other for more than  $10^4$  orbits before merging. The measurements are in good agreement with two-dimensional fluid theory and simulations, and offer an incisive experimental test of these theories since the plasma vortex dynamics is not complicated by the presence of boundary layers at the wall or ends.

We wish to thank Ralph A. Smith and T. M. O'Neil for enlightening discussions. This work was supported by Office of Naval Research Contract No. N00014-89-J-1714 and National Science Foundation Grant No. NSF PHY87-06358.

- 
- [1] Lord Kelvin, in *Mathematical and Physical Papers* (Cambridge Univ. Press, Cambridge, 1910), pp. 155–168.
  - [2] James C. McWilliams, *J. Fluid Mech.* **146**, 21–43 (1984).
  - [3] D. W. Moore and P. G. Saffman, *J. Fluid Mech.* **69**, 465–473 (1975).
  - [4] P. G. Saffman and R. Szeto, *Phys. Fluids* **23**, 2339–2342 (1980).
  - [5] Vernon J. Rossow, *J. Aircr.* **14**, 283–290 (1977).
  - [6] M. V. Melander, N. J. Zabusky, and J. C. McWilliams, *J. Fluid Mech.* **195**, 303–340 (1988).
  - [7] R. W. Griffiths and E. J. Hopfinger, *J. Fluid Mech.* **178**, 73–97 (1987).
  - [8] G. F. Carnevale, P. Cavazza, P. Orlandi, and R. Purini, *Phys. Fluids A* (to be published).
  - [9] J. H. Malmberg, C. F. Driscoll, B. Beck, D. L. Eggleston, J. Fajans, K.S. Fine, X.-P. Huang, and A. W. Hyatt, in *Non-Neutral Plasma Physics*, edited by C. W. Roberson and C. F. Driscoll (American Institute of Physics, New York, 1988), pp. 28–71.
  - [10] C. F. Driscoll, J. H. Malmberg, K. S. Fine, R. A. Smith, X.-P. Huang, and R. W. Gould, in *Plasma Physics and Controlled Nuclear Fusion Research 1988* (IAEA, Vienna, 1989), Vol. 3, pp. 507–514.
  - [11] Y. B. Kim, P. H. Diamond, and H. Biglari, *Phys. Fluids B* **2**, 2143–2150 (1990).
  - [12] R. H. Levy, *Phys. Fluids* **8**, 1288–1295 (1965).
  - [13] C. F. Driscoll and K. S. Fine, *Phys. Fluids B* **2**, 1359–1366 (1990).
  - [14] T. B. Mitchell, C. F. Driscoll, and K. S. Fine, *Bull. Am. Phys. Soc.* **35**, 2135 (1990).
  - [15] K. S. Fine, Ph.D. thesis, University of California, San Diego, 1988 (unpublished).